

Journal of Biomedical Optics

SPIEDigitalLibrary.org/jbo

Underwater near-infrared spectroscopy measurements of muscle oxygenation: laboratory validation and preliminary observations in swimmers and triathletes

Ben Jones
Marco Dat
Chris E. Cooper



Underwater near-infrared spectroscopy measurements of muscle oxygenation: laboratory validation and preliminary observations in swimmers and triathletes

Ben Jones,^{a,*} Marco Dat,^b and Chris E. Cooper^a

^aUniversity of Essex, Centre for Sport and Exercise Sciences, School of Biological Sciences, Wivenhoe Park, Colchester CO4 3SQ, United Kingdom

^bArtinis Medical Systems, A Einsteinweg 17, 6662 PW Elst, The Netherlands

Abstract. The purpose of this research was to waterproof a near-infrared spectroscopy device (PortaMon, Artinis Medical Systems) to enable NIR measurement during swim exercise. Candidate materials were initially tested for waterproof suitability by comparing light intensity values during phantom-based tissue assessment. Secondary assessment involved repeated isokinetic exercises ensuring reliability of the results obtained from the modified device. Tertiary assessment required analysis of the effect of water immersion and temperature upon device function. Initial testing revealed that merely covering the PortaMon light sources with waterproof materials considerably affected the NIR light intensities. Modifying a commercially available silicone covering through the addition of a polyvinyl chloride material (impermeable to NIR light transmission) produces an acceptable compromise. Bland–Altman analysis indicated that exercise-induced changes in tissue saturation index (TSI %) were within acceptable limits during laboratory exercise. Although water immersion had a small but significant effect upon NIR light intensity, this resulted in a negligible change in the measured TSI (%). We then tested the waterproof device *in vivo* illustrating oxygenation changes during a 100 m freestyle swim case study. Finally, a full study compared club level swimmers and triathletes. Significant changes in oxygenation profiles when comparing upper and lower extremities for the two groups were revealed, reflecting differences in swim biomechanics. © The Authors. Published by SPIE under a Creative Commons Attribution 3.0 Unported License. Distribution or reproduction of this work in whole or in part requires full attribution of the original publication, including its DOI. [DOI: 10.1117/1.JBO.19.12.127002]

Keywords: near-infrared spectroscopy; reliability; swimming; triathlete; muscle; waterproof.

Paper 140537R received Aug. 26, 2014; accepted for publication Nov. 12, 2014; published online Dec. 5, 2014.

1 Introduction

Advances in research applications of near-infrared spectroscopy (NIRS) and a developing interest in the sport performance potential of the NIR technique have led to significant advances in NIR technology.^{1,2} Development of portable NIR technology with telemetric capability has taken monitoring of tissue oxygenation and hemodynamics out of the laboratory and into the applied exercise environment. Field-based NIR exercise assessment has already been carried out in a variety of exercise modalities and settings including cycling,³ sprinting,⁴ rowing,⁵ and speed skating.⁶

Obtaining physiological measures during swim exercise presents a greater level of difficulty than terrestrial-based assessment due to the unstable aquatic environment⁷ and the mode of exercise; for example, the concurrent use of the upper and lower body for propulsion in a horizontal position is one of many aspects that separate swimming from most other sports.⁸ Current underwater swim performance assessment has progressed substantially from basic swim time, stroke rate, and count.⁸ Heart rate, blood lactate, and waterproof accelerometer evaluation are now available.^{9,10} Global measures of oxygen consumption (VO₂ max assessment) via Aqua Trainer Valve

Cosmed Technologies© now allows for breath by breath analysis within the pool.^{11,12} However, these assessments are only available during “tethered” swimming, which can interfere with normal swim technique. It has been suggested that when combined with global measures of oxygen consumption a multimodality approach of local and systemic physiological monitoring may provide valuable information that could help to more accurately identify athlete response to workload and also inform exercise prescription.^{13,14} However, little to no research has focused upon the peripheral aerobic parameters associated with swim exercise, and no research has focused upon muscle oxygenation status in or out of the water.

The PortaMon (Artinis Medical Systems) is a miniaturized (83 × 52 × 20 mm), lightweight (84 g), portable NIR apparatus with telemetric capability.¹⁵ Despite technological advancements in device hardware and software capabilities, the PortaMon and other available portable devices are not waterproof; consequently, to date no NIR measurements have been made in water sports. Due to the device size and the ease of device application, it is felt that PortaMon could be a suitable candidate for NIR water-based testing. The light emitting diodes (LEDs) sources can be directly placed onto the skin without the need for optical wiring and fastened cleanly and securely¹⁵ which will allow swim exercise to be performed unencumbered.

Therefore, the aims of this project were to (1) construct a waterproof casing that would protect the PortaMon device,

*Address all correspondence to: Ben Jones, E-mail: bjonesa@essex.ac.uk

(2) assess the effect of the waterproof casing upon device function, (3) assess the effect of water immersion upon device function, (4) ensure the reliability of the results obtained from the modified device, (5) observe preliminary measures of muscle oxygenation during swim exercise. A series of five progressive experiments were carried out to fulfill these aims.

2 Methods

2.1 Testing Optical Effects of Different Waterproof Coverings Using a Tissue Phantom

The portable NIRS apparatus (PortaMon, Artinis, Medical Systems) used in these studies was a dual wavelength continuous wave system, which simultaneously uses the modified Beer–Lambert law and spatially resolved spectroscopy (SRS) methods.² Changes in tissue oxyhemoglobin (O₂Hb), deoxyhemoglobin (HHb), and total hemoglobin (tHb) were measured using the difference in absorption characteristics of wavelengths at 760 and 850 nm. Values for O₂Hb, HHb, and tHb are reported as a change from baseline (30-s averaging before each test) in micromolar units with no presumption of optical path length ($\mu\text{M cm}$). The tissue saturation index (TSI) was expressed in % and calculated as $[\text{O}_2\text{Hb}]/([\text{O}_2\text{Hb}] + [\text{HHb}]) \times 100$. TSI is independent of NIR photon path length in muscle tissue¹⁶ and was calculated using the SRS method.^{17,18} This particular device consists of three light optodes and one detector (Fig. 1), with the interoptode spacing between the light sources and the detector being 30, 35, and 40 mm. Assuming the penetration depth of NIR light into tissue is approximately half the distance between the light sources and detector ~ 2 cm, in fit athletes with a low adipose level, a significant fraction of

light will interrogate the underlying muscle.¹⁹ During all land-based testing, the NIRS system was connected to a personal computer by Bluetooth™ for data acquisition and a sampling rate of 10 Hz was used for analog-to-digital conversion and subsequent analysis.

A variety of commercially available waterproof products such as the aquapac mini waterproof case (Aquapac®, Aquapac International Limited, UK), iSwim waterproof case (Thumbs Up!™ Ltd., UK) and the Design-Go Dry Phone (Design Go Ltd.), designed to encase and protect electronic devices such as mobile phones and cameras, was chosen to assess the PortaMon's utility underwater. These commercial products are predominately made from thermoplastic polyurethane plastic, incorporate silicone or LENZIFLEX™ optically clear windows and are cited as 100% waterproof or carry an ingress protection marking (IPX rating) of 8.

Assessment required an observation of the effect of different waterproof materials upon raw light intensity, the calculated TSI % and quality control factor (QCF) values that are provided by the PortaMon device. The candidate material selection focused on optical clearness, thickness, and bonding qualities. Optical clearness or material transparency was considered as a point of obvious importance, as the transmission of light is most greatly affected by scattering.²⁰ Any additive effect to scattering through material opacity would greatly alter the intensity of light transmission. Material thickness and robustness were also considered, as thin materials would be unlikely to remain waterproof during dynamic exercise assessment, and materials too thick would reduce the NIR penetration depth into sample tissue. Assessment was achieved by making a direct comparison between placing the PortaMon device onto an optical phantom block with and without the different waterproof material

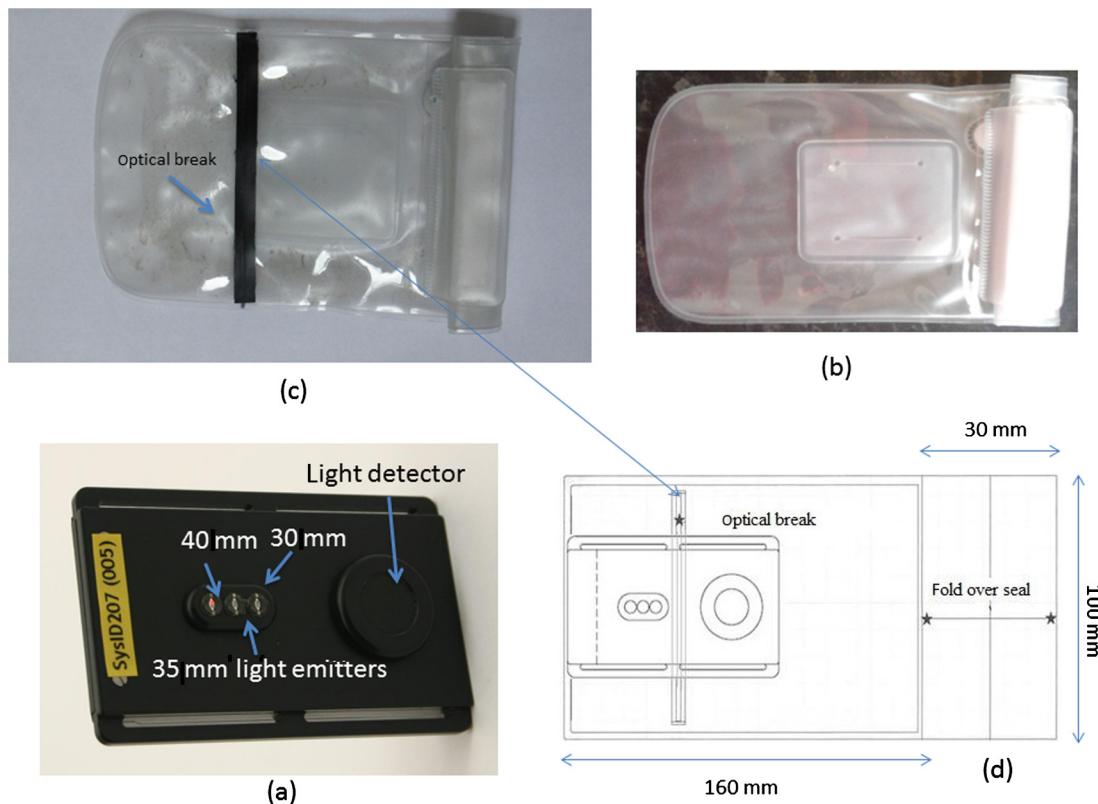


Fig. 1 PortaMon-portable dual wavelength continuous wave near-infrared device (a), iSwim waterproof covering before (b) and after modification (c) with technical outlay drawing describing the modification (d).

coverings. The tissue phantom was made as described previously²¹ (μ_a at 800 nm = 0.01 mm⁻¹).

The TSI provided by the PortaMon is a measurement of tissue oxygen saturation (StO₂), which can specify the extent to which blood is oxygenated.^{16,17} TSI is the SRS-derived approximation of StO₂—the concentration of oxyhemoglobin (O₂Hb) relative to the total concentration of hemoglobin [O₂Hb + HHb (deoxyhemoglobin)].¹⁸ Normal physiological TSI (%) readings within skeletal muscle would be in the region of ~60% to 80%, although this number will vary between individuals and greatly change during dynamic exercise.²² In contrast, a TSI (%) measurement from an optical phantom provides a robust, reproducible, and stable number.

To calculate the TSI, the SRS method measure assumes a linear relationship between the optical densities and the source: detector distance for each wavelength. The PortaMon uses three distances to estimate this slope and provides a QCF to estimate the linearity of the relationship. QCF is calculated using the standard error propagation rule using the slope for both wavelengths. The given QCF value is high (maximum 100%) when the measurement fits the linear assumption.

2.2 Testing During Exercise

A repeated isometric quadriceps contraction exercise task was implemented to determine the effect and accuracy of the waterproof covering upon device function and NIRS variables during a standard exercise test. Eight recreationally active subjects, six male and two female; mean \pm SD = age 23.6 \pm 5.3 years; weight 80.6 \pm 10.4 kg; height 176.1 \pm 9.5 cm; vastus lateralis skinfold 11.6 \pm 5.0 mm participated in this study. All subjects had no known health problems or any lower limb muscle or joint problems (Par-Q). Subjects were asked not to perform any strenuous activity 24 h prior to each experimental visit. The study received ethical approval (University of Essex ethical committee) and all subjects provided written consent.

The experimental protocol involved five visits to the University of Essex biomechanics lab. The first enabled subjects to become familiar with the data collection procedures and allowed the assessment of descriptive statistics. The thickness of adipose tissue overlaying the quadriceps muscle was measured using a skinfold caliper (British Indicators, Harpenden, UK) and maximal voluntary contraction (MVC) of the knee extensors was measured with a dynamometer (KinCom, Chattex; Chattanooga, TN). All subjects performed a nonspecific light warm up on a cycle ergometer (Monark, 824E). Subjects were securely attached to isokinetic dynamometer using both a waist and upper body strapping attachment to minimize any upper body contribution to the quadriceps contraction. The dominant leg was then selected and fixed at a 60 deg angle and three repetitions of a 5 s continuous maximal isometric contraction with a 60-s rest period were performed. The strongest contraction of the three repetitions was then taken as the maximal isometric force. Values for 10%, 30%, and 50% MVC were then calculated. On the second and third visits the subject was required to perform a series of 30 s sustained isometric quadriceps contractions to the previously defined values of their MVC followed by a 3-min period of rest; at 10% of MVC, 30% MVC, and finally at 50% MVC. During the second and third visits, the PortaMon device was positioned on the belly of the vastus lateralis muscle, midway between the greater trochanter of the femur and the lateral femoral epicondyle. To ensure the optodes and detector remained in position relative to

the subject's skin, the device was fixed into position using tape and secured with a black neoprene strap. During the fourth and fifth visits to the lab, the same protocol was repeated but with the PortaMon device encased in the previously designed waterproof casing. To ensure accuracy of repeat device placement, an outline of the device was drawn onto each subject's leg. Subjects were asked to maintain the outline during the testing period. Additionally, any bodily hair within the probe placement area was removed from each subject's skin and subjects were asked not to use any moisturizing products on the testing day. The same researcher attached each device and applied the sports strapping, asking the subjects if the device and strapping felt comfortable and secure. All visits were at intervals of between 3 and 5 days and testing was performed at the same time of day.

Values for O₂Hb, HHb, and tHb are reported using the same methodology previously described in Sec. 2.1. The TSI % was calculated using SRS methods. Maximum and minimum TSI % values were calculated as a 1-s average surrounding the highest and lowest values during each of the three 30 s isometric holds. The Δ in TSI was, therefore, calculated as the maximum value minus the minimum value during each sustained contraction, e.g., TSI Max – TSI Min = Δ TSI.

Descriptive statistics are presented as a mean \pm SD unless otherwise stated. Accuracy was calculated as the mean absolute difference, using Bland–Altman agreements plots (\pm 2SD) between the change in Δ TSI% measurements, during 10%, 30%, and 50% MVCs. The 95% confidence interval of the mean (95%CL) is also presented for each case.^{23,24} A repeated measures analysis of variance (ANOVA) was carried out to compare the reproducibility of the mean torque and Δ TSI values across the four exercise sessions. Furthermore, a coefficient of variance (CV) was calculated for each subject across the four sessions, and the mean value of the subjects was used as an indicator of the test-retest reliability for TSI (%) and torque (*N*) variables. All analyses were performed using Graphpad Prism 6 (Graphpad Software, San Diego, CA).

2.3 Testing Optical Effects During Water Immersion

In order to assess the effect of both water immersion and water temperature upon the PortaMon device function, testing was conducted upon emitted light intensity changes, TSI % and QCF values when the PortaMon device, covered by a specially modified, commercially available, waterproof covering, was out of water at ambient temperature (20°C) and then, during water immersion at temperatures of 30°C, 20°C, 10°C, respectively. Light intensity values were recorded for 10 min, with average intensity values logged. The PortaMon device was attached to a tissue phantom as described previously²¹ (μ_a at 800 nm = 0.01 mm⁻¹) and covered with a black covering to prevent ambient light interference. Water temperature was monitored using a water-based thermometer (ET402/Emerson Electronic, Reading, UK). Crushed ice was administered to lower the water temperature. Descriptive statistics are presented as a mean \pm SD unless otherwise stated. Each variable was examined with Kolmogorov–Smirnov normality test. A one-way repeated measures ANOVA was used to compare the differences between the out-of-water light intensities for each LED and also at each water temperature when immersed. The level of significance for analyses was set at $p < 0.05$. All analyses were performed using Graphpad Prism 6 (Graphpad Software, San Diego, CA).

2.4 Testing During Swimming

An assessment of PortaMon utility and function during an underwater swim test upon skeletal muscle was conducted during an individual case study. A 23-year-old recreationally active male (height 176 cm; weight 69 kg; vastus lateralis skinfold 6 mm) completed a 100 m maximal effort freestyle swim. The PortaMon device was positioned on the belly of the vastus lateralis muscle, midway between the greater trochanter of the femur and the lateral femoral epicondyle. To ensure the optodes and detector did not move relative to the subject's skin, the device was fixed into position using sports adhesive tape and secured with a black sports support strapping to prevent contamination from ambient light. During underwater testing, the bluetooth function was not possible; subsequently the PortaMon stored the data within the device's internal memory capacity. These data were then downloaded onto a personal computer for data analysis through an online software program. The subject passively stood in the shallow end of the swimming pool (waist immersion), with his arms by his sides and his body weight evenly distributed over each leg, for a 2-min period to establish a baseline reading. The subject then started freestyle swimming without diving from the pool edge and did not perform regular ("tumble turn") turning motions at the end of the lane, but instead briefly touched the pool edge and resumed swimming immediately without gliding underwater after the turn. The restriction placed on the typically performed "tumble turn" was implemented to reduce pressure on the device's attachment. The subject completed 4 × 25 m lengths of a short-course swimming pool at a maximal pace. Upon completion the subject passively stood for 2 min at the shallow end of the pool, following the same procedure as for the baseline attainment. Values for O₂Hb, HHb, and tHb are reported as a change from baseline (30-s averaging before the start of the test) in micromolar centimeter units (μM cm). The TSI (%) was also calculated following the same procedure as Sec. 2.1.

2.5 Comparing Differences in Swim Technique in Athletes and Triathletes

Two subgroups of swim athletes consisting of 10 subjects—five club level swimmers and five club level triathletes (3 men and 7 women)—were tested. Swim group (mean ± SD = age 21.2 ± 1.6 years; height 170.6 ± 7.5 cm; weight 62.8 ± 6.9 kg; vastus lateralis skin fold 13.8 ± 5.6 mm, latissimus dorsi (LD) 12.6 ± 3.7). Triathlete group (mean ± SD = age 44.0 ± 10.5 years; height 171.6 ± 7.0 cm; weight 68.6 ± 12.7 kg; vastus lateralis skin fold 11.8 ± 3.5 mm, LD 11.2 ± 3.1).

Two PortaMon devices were positioned on the belly of the vastus lateralis muscle (as described in Sec. 2.4) and at the LD muscle at the midpoint between the midaxilla and the spinal column. Each subject was then asked to perform a maximal 200 m freestyle swim (8 × 25 m). The swim protocol, baseline, and recovery procedures are the same as described in Sec. 2.4. To ensure the optodes and detector did not move relative to the subject's skin, the device was fixed into position using sports waterproof adhesive tape and secured using the subject's own specialist swim apparel. NIRS measurements are the same as those reported in Sec. 2.4. Descriptive statistics are presented as a mean ± SD unless otherwise stated. Each variable was examined with Kolmogorov–Smirnov normality test. ΔTSI% between the vastus lateralis and LD were analyzed using either paired (2-tailed) *t*-tests or Wilcoxon signed rank test when the sample normality test failed as per Bravo et al.²⁵ The level of significance for analyses was set at *p* < 0.05. All analyses were performed using Graphpad Prism 6 (Graphpad Software, San Diego, CA).

3 Results

3.1 Testing Optical Effects of Different Waterproof Coverings

Initial testing revealed that merely covering the PortaMon light sources with waterproof materials considerably affected the NIR light intensities at the detector (Table 1). The results in Table 1

Table 1 Comparison of PortaMon TSI (%), quality control factor (QCF), and light intensities when covered with waterproof materials.

Material	TSI %	QCF	Light intensities					
			Emitter 1		Emitter 2		Emitter 3	
			(1) 844 nm (30 mm)	(2) 762 nm (30 mm)	(1) 854 nm (35 mm)	(2) 763 nm (35 mm)	(1) 847 nm (40 mm)	(2) 769 nm (40 mm)
Phantom alone	62	99.83	1.034	1.256	1.556	1.809	2.028	2.274
+ Cling film	61	99.77	1.033	1.252	1.563	1.809	2.021	2.270
+ Latex glove	65	99.83	1.061	1.285	1.581	1.835	2.047	2.298
+ Silicone 0.50 mm	85	95.60	0.236	0.468	1.078	1.212	1.438	1.572
+ Silicon-0.25 mm	80	99.04	0.891	1.074	1.355	1.539	1.710	1.849
+ PVC	67	99.67	0.770	0.930	1.291	1.472	1.735	1.911
+ Aquapac	65	95.60	0.469	0.596	1.424	1.615	1.887	2.058
+ iSwim	100	95.95	0.827	0.962	1.268	1.389	1.529	1.554

Once a material is placed over the light source, light source intensity, TSI %, and QCF values are considerably altered. The uncovered phantom acts as a baseline comparison value (**highlighted in bold**). Light intensity values are presented as optical density (OD) units.

Table 2 Comparison of PortaMon TSI (%), QCF, and light intensities when covered with waterproof materials incorporating a near-infrared opaque layer.

Material	TSI%	QCF	Light intensities					
			Emitter 1		Emitter 2		Emitter 3	
			(1) 844 nm (30 mm)	(2) 762 nm (30 mm)	(1) 854 nm (35 mm)	(2) 763 nm (35 mm)	(1) 847 nm (40 mm)	(2) 769 nm (40 mm)
Phantom alone	61	99.88	0.955	1.249	1.469	1.800	1.935	2.279
+ Clingfilm	63	99.88	1.059	1.281	1.580	1.834	2.055	2.314
+ Silicone-0.50 mm	69	99.17	0.910	1.130	1.541	1.767	2.000	2.230
+ Silicone-0.25 mm	67	99.56	0.768	0.939	1.395	1.587	1.898	2.092
+ iSwim	62	99.87	0.984	1.274	1.468	1.784	1.902	2.225

The phantom acts as a baseline comparison value (**highlighted in bold**). Candidate material iSwim; a commercially available, silicone-based material, produced comparable results to phantom (**highlighted in bold**). Light intensity values are presented as OD units.

report higher light intensities when the device is covered, with the exception of cling film and latex. Both these materials are able to make a tight seal, but are thin and unlikely to be robust enough for the physical demands of the exercise protocols. However, the more robust materials, as well as allowing excess light to reach the detector, showed a marked nonlinearity in the optical density (OD) change with respect to distance, as evidenced by a drop in the QCF. Taken together these effects suggest that a significant fraction of the light reaching the detector is not passing through the tissue. The most likely explanation is that reflected light is “piping” along the surface of the waterproof coverings and, therefore, being detected by the light receiver without entering the target tissue. In an attempt to correct this, the candidate materials were cut in half and bonded back together incorporating a black polyvinyl chloride (PVC) NIR opaque layer as an optical break (Fig. 1). Subsequent results (Table 2) showed a significant improvement in TSI (%), QCF, and light attenuation.

3.2 Testing During Exercise

Similar patterns of change in tHb, O₂Hb, HHb, and TSI (%) were seen in all eight subjects during the three sets of isometric voluntary quadriceps muscle contraction at 10%, 30%, and 50% MVC.

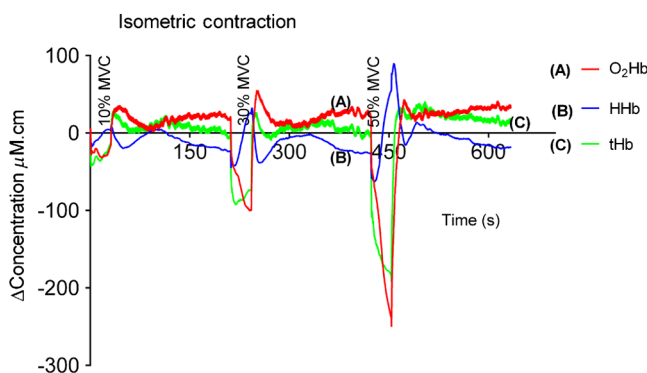


Fig. 2 Group changes in oxyhemoglobin (ΔO_2Hb), deoxyhemoglobin (ΔHHb), and total hemoglobin (ΔtHb) during 10%, 30%, and 50% isometric maximal voluntary contraction (MVC) tasks.

MVC. Figure 2 is a composite graph of the group averaged data which shows the pattern of change in chromophore concentration (O₂Hb and HHb) and tHb observed during the testing protocol. The changes in TSI (%) are shown in Fig. 3 on the same timescale.

The average absolute difference between $\Delta TSI\%$ (PortaMon versus PortaMon and Covering) at baseline, 10%, 30%, and 50% MVC were 0.75 ± 2.49 , $CL = -4.13$ to 5.56 ; 0.08 ± 0.45 , $CL = -0.80$ to -0.96 ; 0.80 ± 2.45 , $CL = -4.06$ to 5.68 ; 0.17 ± 2.01 , $CL = -4.11$ to 3.77 . Bland-Altman plots (Fig. 4) illustrate these effects and also indicate that there is no trend to a less accurate measurement as the signal size increases.

Table 3 displays average torque (N) and ΔTSI values during baseline 10%, 30%, and 50% MVC tasks and their associated CV. It is clear that adding the waterproof covering does not add significant variability over and above that due to normal physiology and exercise testing procedures.

3.3 Testing Optical Effects During Water Immersion

Table 4 shows the light intensity changes, TSI %, and QCFs values averaged over a 10-min period at room temperature (out of water) and at 30°C, 20°C, and 10°C, respectively, when immersed in water. There is a significant ($p < 0.05$) reduction in average light intensity detected for all emitters when the

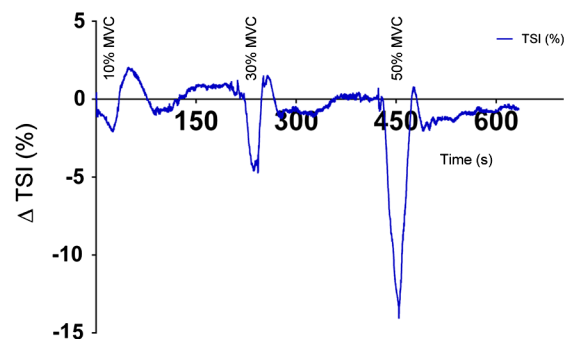


Fig. 3 Group changes in tissue saturation index ($\Delta TSI\%$) during 10%, 30%, and 50% isometric MVC tasks.

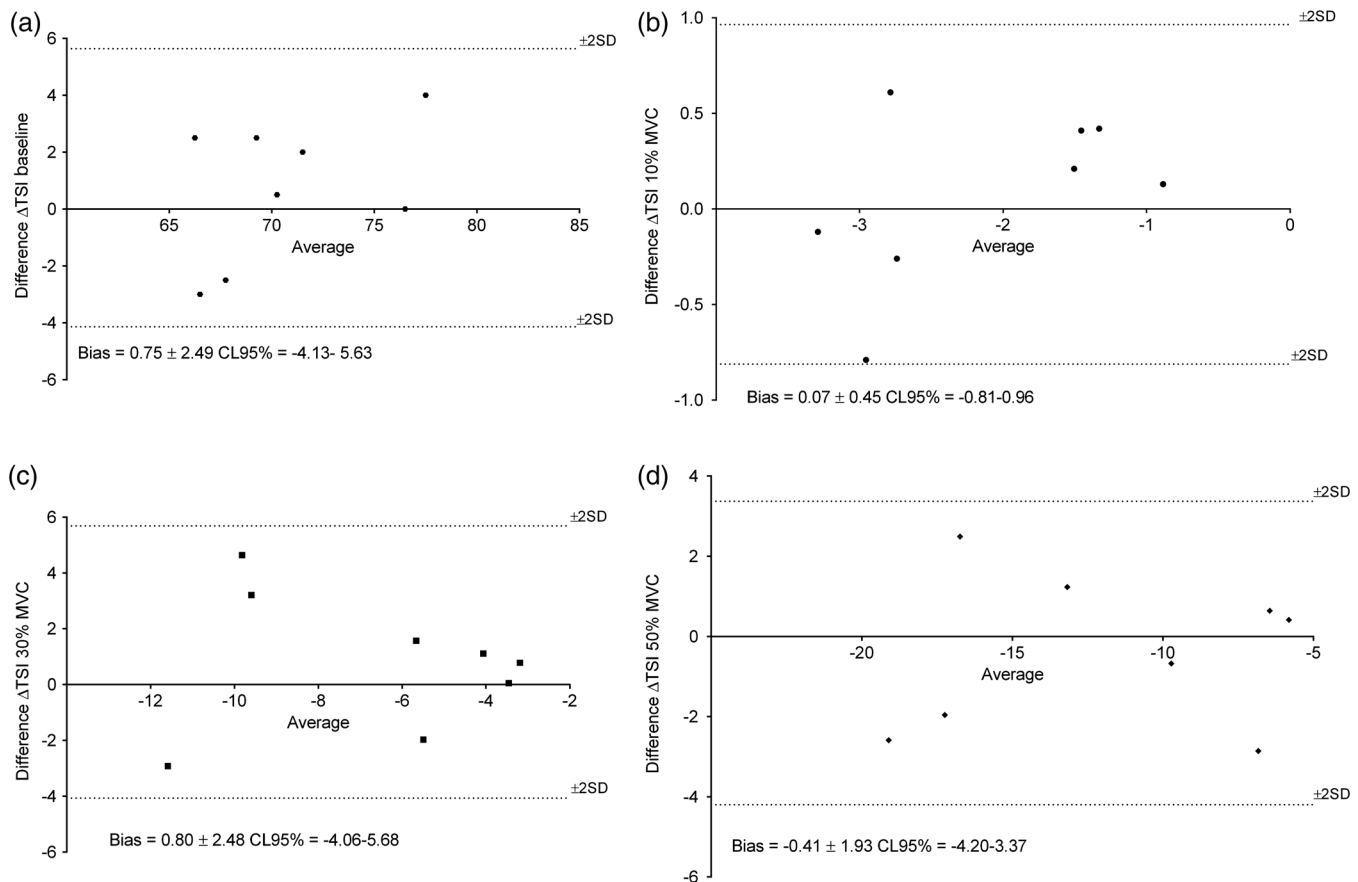


Fig. 4 Bland–Altman plots of Δ TSI at baseline (a) and for the three 30 s sustained isometric contraction tasks at 10% (b), 30% (c), and 50% (d) MVC. Each plot represents the difference versus mean Δ value measured as the average of the two uncovered compared to the two covered tests. Dotted lines represent the ± 2 SD limits of agreement.

Table 3 Average torque (N) integral and vastus lateralis tissue saturation index (Δ TSI%). Mean \pm SD ($n = 8$).

	Uncovered	Uncovered	Covered	Covered	CV (%)
Torque 10%	56.4 \pm 9.7	55.0 \pm 9.8	54.4 \pm 12.8	56.1 \pm 10.9	4.31 \pm 3.43
Torque 30%	156.7 \pm 32.0	157.7 \pm 35.5	155.4 \pm 32.16	155.0 \pm 31.8	2.80 \pm 0.96
Torque 50%	257.6 \pm 52.1	253.8 \pm 54.7	253.4 \pm 52.1	257.1 \pm 54.1	1.83 \pm 1.45
Baseline TSI%	71.0 \pm 6.2	71.1 \pm 4.2	70.4 \pm 3.9	70.3 \pm 4.3	2.8 \pm 1.3
10% MVC TSI%	68.8 \pm 6.8	69.2 \pm 4.6	68.1 \pm 4.8	68.2 \pm 4.7	7.7 \pm 1.5
30% MVC TSI%	64.5 \pm 8.2	65.2 \pm 6.3	64.0 \pm 6.7	62.6 \pm 7.8	11.3 \pm 1.5
50% MVC TSI%	58.9 \pm 9.8	59.0 \pm 8.3	58.7 \pm 8.1	58.5 \pm 8.4	14.7 \pm 1.3

The mean torque integral during the 10%, 30%, and 50% MVC did not change significantly ($p > 0.05$) across the four sessions and the CVs were less than 5%. Absolute TSI % numbers are presented. The ANOVA showed no significant differences in TSI measures ($p > 0.05$). Baseline Δ TSI% provided a reproducible number across the four testing sessions. Larger variability in the Δ TSI% was seen during exercise, with the greatest variance observed during the higher exercise intensities.

PortaMon device is immersed in water (Table 4). However, there is no significant difference in light intensity values when the device is immersed at the different water temperatures ($p > 0.05$) (30°C, 20°C, or 10°C). The observed change in light intensity results in only a very small/negligible change in TSI (%) and QCF values.

3.4 Testing During Swimming

Figures 5 and 6 show the changes in hemoglobin and TSI variables during a 100 m freestyle swim, respectively. As the swim starts, a clear drop in O_2 Hb (max drop $\Delta - 382.9 \mu\text{M cm}$) is evident concomitant with an increase in HHb (max increase

Table 4 Average light intensity values at all temperatures.

Temperature (°C)	TSI%	QCF	Light intensities					
			Emitter 1		Emitter 2		Emitter 3	
			(1) 844 nm (30 mm)	(2) 763 nm (30 mm)	(1) 845 nm (35 mm)	(2) 763 nm (35 mm)	(1) 846 nm (40 mm)	(2) 765 nm (40 mm)
Out of water 20°C	63	99.39	1.069	1.310	1.578	1.848	1.976	2.248
Immersed 30°C	64	99.65	1.121	1.353	1.603	1.868	2.016	2.270
Immersed 20°C	64	99.56	1.123	1.351	1.616	1.880	2.027	2.280
Immersed 10°C	64	99.48	1.121	1.350	1.614	1.881	2.021	2.274

There is a significant difference between out-of-water versus water immersion ($p < 0.05$). There is no significant difference between light intensity detected at the receivers at 30°C, 20°C, and 10°C ($p > 0.05$). Light intensity values are presented as OD units.

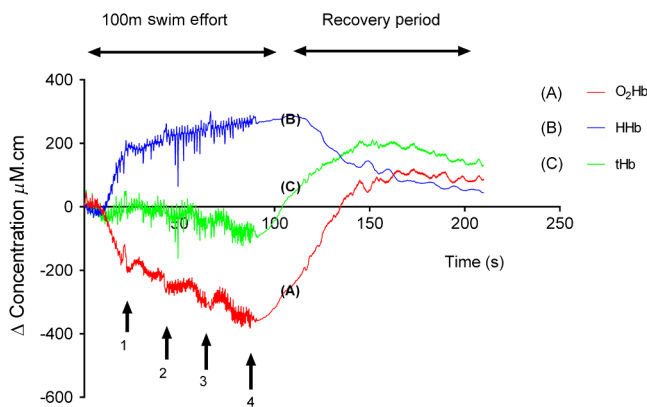


Fig. 5 Changes seen in hemoglobin variables during a 100 m freestyle swim effort.

$\Delta + 301.14 \mu\text{M}\cdot\text{cm}$) while the tHb remained relatively unchanged. Both O₂Hb and HHb readings continue to, respectively, drop and increase throughout the $4 \times 25\text{-m}$ lengths [as indicated by the numbers (1 to 4) marking the end of each 25-m length]. During the recovery period, a large increase in tHb is evident, indicative of the hyperemic response which is commonly seen following dynamic exercise. TSI (%) progressively drops throughout the swim period (max drop $\Delta - 38\%$). Following cessation of the swim exercise, TSI (%) increasingly

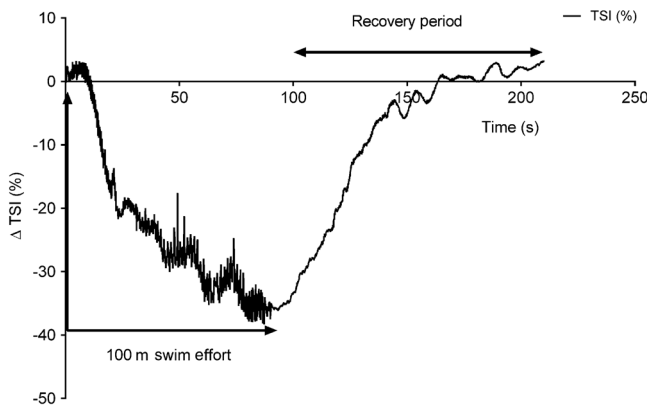


Fig. 6 Changes seen in $\Delta\text{TSI}(\%)$ during a 100 m freestyle swim.

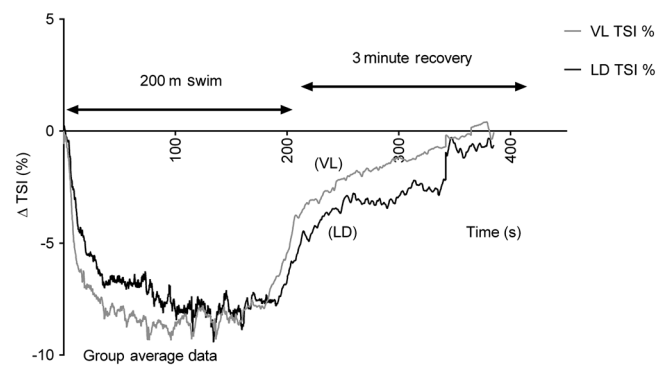


Fig. 7 Swim group $\Delta\text{TSI}\%$ of the vastus lateralis and latissimus dorsi (LD) during 200 m freestyle swimming.

returns to baseline levels during the recovery period. The QCF value additionally remained high throughout the swim test (99.8%). The swimmer indicated minimal discomfort when wearing the device and the machine itself was undamaged by the procedure.

3.5 Comparing Differences in Swim Technique in Athletes and Triathletes

Figures 7 and 8 show the $\Delta\text{TSI}\%$ trend for swim and triathlon groups measured at the vastus lateralis (VL, quadriceps, leg) and

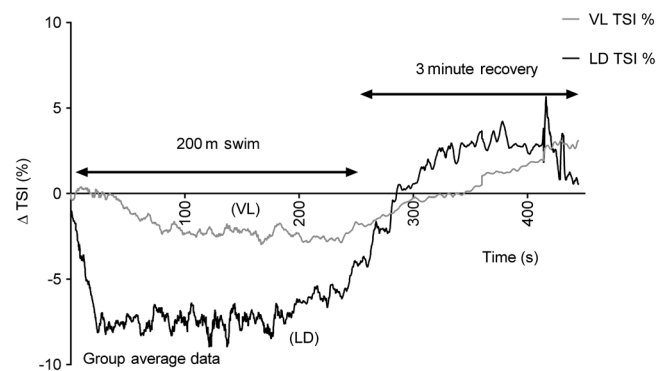


Fig. 8 Triathlon group $\Delta\text{TSI}\%$ of the vastus lateralis and LD during 200 m freestyle swimming.

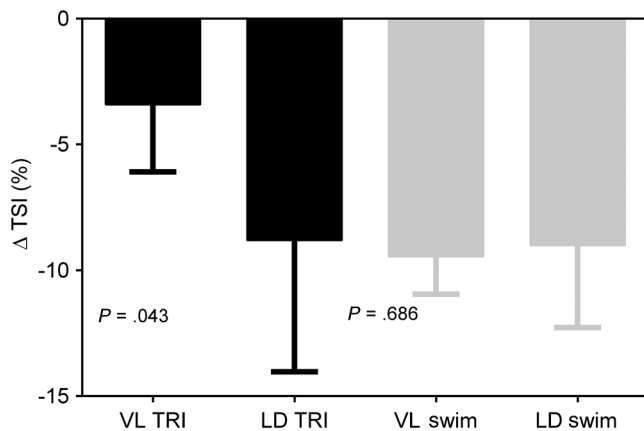


Fig. 9 Club level swimmer and club level triathlete group average Δ TSI (%) in the vastus lateralis and LD muscles during a maximal 200 m freestyle swim effort ($n = 10$).

LD (shoulder/back) during a 200 m freestyle swim. At the onset of exercise in the club level swimmer group, there is a rapid drop in TSI in both the VL and LD during the first 50 s; thereafter, the TSI reaches a plateau for the remainder of the swim effort. In contrast, in the club level triathlete group, at the onset of exercise there is a rapid drop in TSI in the LD, but not the VL muscle. Recovery of LD TSI is seen during the postswim recovery period. The TSI of the VL remains relatively stable with small increases and decreases seen during the initial part of the swim. Toward the end of the swim effort, a gradually greater decrease is seen, with recovery occurring predominantly in the postswim recovery period. Importantly, QCF values for the TSI (%) measures remained above 98% for all swim athletes in both the VL and LD muscle groups, indicating a high level of measurement consistency. Figure 9 summarizes the group data, illustrating the significant difference between leg and trunk muscle deoxygenation during swimming in those athletes who train for triathlons, as opposed to those who only train for swimming.

4 Discussion

This is the first study to report on peripheral muscle oxygenation changes during swim exercise using a specially modified portable NIR device. The main findings from the current studies are below.

4.1 Testing Optical Effects of Different Waterproof Coverings

Simply covering the PortaMon device in a waterproof sheath will prevent the device from functioning properly. Modifying an optically clear, transparent, commercially available silicone covering through the application of a bonded, thin, black PVC material, which is impermeable to NIR light transmission, produces an acceptable compromise.

4.2 Testing During Exercise

The main findings from this study were that the addition of the waterproof covering added no significant variability to the TSI % measures during a controlled exercise task. Absolute measurement of individual subject variability as demonstrated by Bland-Altman \pm 2SD limits of agreement were within acceptable limits.²⁶ CV data revealed consistent force production throughout all exercise tasks and CV values for baseline and

Δ TSI (%) were comparable with previously reported values during isokinetic laboratory-based exercise tasks.²⁷ This study, therefore, validated the use of a waterproof covering for subsequent swim-based exercise monitoring and assessment.

4.3 Testing Optical Effects During Water Immersion

Results indicated a significant reduction in PortaMon light intensity detected when the device was immersed in water. Potential explanations could relate to either a small amount of water coming between the waterproof material covering the light sources and the phantom surface and/or an increase in surface pressure upon the device leading to an increase in the sampled area. However, it should be noted the intensity change resulting from the water immersion had only a negligible effect on the derived TSI and QCF values. It has previously been suggested that a change in water temperature may have an additional effect on the temperature of the LEDs^{28,29} and, therefore, result in an alteration of wavelength values, which would potentially affect perceived oxygen levels. However, apart from the effects of the initial water immersion, there was no significant effect of water temperature upon any NIRS measured parameter on an optical phantom.

4.4 Testing During Swimming

The main outcome from this case study is that the waterproofed PortaMon was able to successfully monitor hemoglobin variables underwater during a dynamic 100 m swim effort. During the 100 m swim both O_2 Hb and TSI (%) progressively decreased during each 25 m length, with a subsequent increase in HHb while the tHb remained largely unchanged. At the end of the exercise, both TSI% (Fig. 6) and O_2 Hb recovered, with an increase in tHb and decrease in HHb (Fig. 5). These observed changes in hemoglobin and muscle oxygen responses during dynamic swim exercise and the hyperaemic response (increase in tHb above resting level) observed during the postswim recovery period have been previously reported during dynamic land-based exercise,³⁰ where NIRS technology has been utilized to record measurements. The similarity between both our aquatic study and the aforementioned land-based exercise observations using NIRS measurements is positive and bodes well for the feasibility of our modified waterproof covering. In some cases, relatively large fluctuations in the NIRS signals (Figs. 5 and 6) were seen during swim testing. Postswim communication with the subject revealed that the device felt progressively loose under the sports strapping during the swim exercise. This movement artifact could explain some of the noise in the data signal. The use of sports waterproof taping and specific swim apparel greatly reduced this effect as seen in the NIRS signal traces (Figs. 7 and 8) in the subsequent (Sec. 4.5) swim study.

4.5 Comparing Differences in Swim Technique in Athletes and Triathletes

This NIRS study is the first to compare oxygenation changes in real time in muscle groups during swimming. In freestyle swimming, >85% of the thrust is gained from the upper body.³¹ However, triathlete's and swimmers vary in swim velocity and propulsion efficiency.³² Visual inspection of the athletes in our study indicated this contrast. The club level swimmers used both upper body and lower body for propulsion during maximal

intensity swimming. However, even when told to swim as fast as possible, triathletes used only the upper body presumably due to the need to spare the leg muscles for the later cycling and running stages of their event. The NIRS data reflected these biomechanical differences. The $\Delta\text{TSI}\%$ changes indicated that club level swimmers use both the upper and lower muscles to a similar extent during a maximal 200 m swim, whereas there was minimal desaturation in the lower body muscles of the triathletes.

To conclude, wider applications of this new waterproof technology could lead to effective, noninvasive monitoring of hemoglobin variables during swim exercise, allowing the swim coach and/or exercise physiologist to observe the relative contributions of muscles during swim exercise. This may well enable a greater understanding of the differences in swimming techniques seen in individual swimmers. Additionally, NIRS measurements can be utilized during specific swim training periods such as early season, aerobic, high volume training or when a training emphasis is placed upon the upper or lower body. During such training, NIRS offers the potential to report upon peripheral measurements of muscle oxygenation that are indicative of adaptive local responses to training.³³ In conjunction with this, it has been suggested that a local measurement of muscle oxygenation during swim exercise would contribute to a multimodality approach that is perhaps warranted to enable a more detailed evaluation of swim athletes,¹³ and complement the global measurements of oxygen consumption that are already attainable. Furthermore, this technology can be applied to other open water sports such as rowing, canoeing, and windsurfing.

There may be therapeutic applications of this technology. Cold water immersion therapy (CWIT) is a commonly practiced recovery intervention, utilized across multisports.³⁴ The efficacy of this modality and the scientific principles involved are yet to be fully explained.³⁵ Recently, NIRS has been experimentally trialed by research groups in an attempt to identify hemodynamic responses during such muscle cooling techniques.³⁶ However, full body immersion protocols have not been possible due to the lack of waterproof capable devices.³⁷ The hydrostatic pressure effect of immersion is suggested as one of the key mechanisms behind the benefits of CWIT practice³⁸ and the development of this waterproof covering will enable further assessment of this modality.

Finally, the results from the current collection of studies show that the acquisition of a peripheral measurement of muscle oxygenation is possible using a specially modified waterproof covering over an existing portable NIR device. The reliability of the obtained results using the waterproof covering, as represented through absolute measurement error using Bland-Altman plots, were found to be within acceptable limits. The measurements of muscle oxygenation seen in an individual subject and in club level swimmers and triathletes illustrate the ability of NIRS to detect hemodynamic changes in difficult environments.

Acknowledgments

We acknowledge helpful discussions with Dr. Terrence Leung at the Department of Medical Physics and Bioengineering, University College London and the same department for the loan of the tissue phantom. The work described here was funded in part by grant EP/F005733/1 from the UK Engineering and Physical Sciences Research Council (EPSRC). The authors report that there were no conflicts of interest for this paper.

Disclaimer: Marco Dat, a coauthor of this paper and an employee Artinis Medical systems contributed towards results interpretation and discussion; however, in no way do the findings of this paper constitute endorsement of the PortaMon device by the authors or the Journal of Biomedical Optics.

References

1. A. Macnab and B. Shadgan, "Biomedical applications of wireless continuous wave near infrared spectroscopy," *Biomed. Spectrosc. Imaging* **1**(3), 205–222 (2012).
2. M. Ferrari, M. Muthalib, and V. Quaresima, "The use of near-infrared spectroscopy in understanding skeletal muscle physiology: recent developments," *Philos. Trans. R. Soc. A* **369**(1955), 4577–4590 (2011).
3. J. P. Neary, D. C. McKenzie, and Y. N. Bhambhani, "Effects of short-term endurance training on muscle deoxygenation trends using NIRS," *Med. Sci. Sports Exerc.* **34**(11), 1725–1732 (2002).
4. P. Ufland et al., "Reproducibility and sensitivity of muscle reoxygenation and oxygen uptake recovery kinetics following running exercise in the field," *Clin. Physiol. Funct. Imaging* **31**(5), 337–346 (2011).
5. B. Chance et al., "Recovery from exercise-induced desaturation in the quadriceps muscles of elite competitive rowers," *Am. J. Physiol.* **262**(3), C766–C775 (1992).
6. C. M. Hesford et al., "Asymmetry of quadriceps muscle oxygenation during elite short-track speed skating," *Med. Sci. Sports Exerc.* **44**(3), 501–508 (2012).
7. D. R. Pendergast and C. E. Lundgren, "The underwater environment: cardiopulmonary, thermal, and energetic demands," *J. Appl. Physiol.* **106**(1), 276–283 (2008).
8. D. J. Smith, S. R. Norris, and J. M. Hogg, "Performance evaluation of swimmers," *Sports Med.* **32**(9), 539–554 (2002).
9. T. Barbosa et al., "Kinematical changes in swimming front Crawl and Breaststroke with the AquaTrainer® snorkel," *Eur. J. Appl. Physiol.* **109**(6), 1155–1162 (2010).
10. O. Keskinen, K. Keskinen, and A. Mero, "Effect of pool length on blood lactate, heart rate, and velocity in swimming," *Int. J. Sports. Med.* **28**(5), 407–413 (2007).
11. V. Reis et al., "Examining the accumulated oxygen deficit method in front crawl swimming," *Int. J. Sports. Med.* **31**(6), 421–427 (2010).
12. M. Pinna et al., "Assessment of the specificity of cardiopulmonary response during tethered swimming using a new snorkel device," *J. Physiol. Sci.* **63**(1), 7–16 (2013).
13. J. F. Reis et al., "Effects of aerobic fitness on oxygen uptake kinetics in heavy intensity swimming," *Eur. J. Appl. Physiol.* **112**(5), 1689–1697 (2012).
14. B. Wang et al., "Comparisons of local and systemic aerobic fitness parameters between finswimmers with different athlete grade levels," *Eur. J. Appl. Physiol.* **112**(2), 567–578 (2012).
15. B. Shadgan et al., "Wireless near-infrared spectroscopy of skeletal muscle oxygenation and hemodynamics during exercise and ischemia," *Spectroscopy* **23**(5–6), 233–241 (2009).
16. M. Wolf, M. Ferrari, and V. Quaresima, "Progress of near-infrared spectroscopy and topography for brain and muscle clinical applications," *J. Biomed. Opt.* **12**(6), 062104 (2007).
17. M. S. Patterson, B. Chance, and B. C. Wilson, "Time resolved reflectance and transmittance for the non-invasive measurement of tissue optical properties," *Appl. Opt.* **28**(12), 2331–2336 (1989).
18. S. Suzuki et al., "Tissue oxygenation monitor using NIR spatially resolved spectroscopy," *Proc. SPIE* **3597**, 582–592 (1999).
19. M. Ferrari, L. Mottola, and V. Quaresima, "Principles, techniques, and limitations of near infrared spectroscopy," *Can. J. Appl. Physiol.* **29**(4), 463–487 (2004).
20. P. D. Mannheim, "The light-tissue interaction of pulse oximetry," *Anesth. Analg.* **105**(On Line Suppl.), S10–S17 (2007).
21. M. Firbank, M. Oda, and D. T. Delpy, "An improved design for a stable and reproducible phantom material for use in near-infrared spectroscopy and imaging," *Phys. Med. Biol.* **40**(5), 955 (1995).
22. V. Quaresima, R. Lepanto, and M. Ferrari, "The use of near infrared spectroscopy in sports medicine," *J. Sports Med. Phys. Fitness* **43**(1), 1–13 (2003).

23. A. M. Batterham and W. G. Hopkins, "Making meaningful inferences about magnitudes," *Int. J. Sports Physiol. Perform.* **1**(1), 50–57 (2006).
24. W. Hopkins et al., "Progressive statistics for studies in sports medicine and exercise science," *Med. Sci. Sports Exerc.* **41**(1), 3–12 (2009).
25. D. M. Bravo et al., "Skeletal muscle reoxygenation after high-intensity exercise in mitochondrial myopathy," *Eur. J. Appl. Physiol.* **112**(5), 1763–1771 (2012).
26. M. J. Bland and D. G. Altman, "Statistical methods for assessing agreement between two methods of clinical measurement," *Lancet* **327**(8476), 307–310 (1986).
27. M. Muthalib et al., "Reliability of near-infrared spectroscopy for measuring biceps brachii oxygenation during sustained and repeated isometric contractions," *J. Biomed. Opt.* **15**(1), 017008 (2010).
28. S. Muthu, F. J. Schuurmans, and M. D. Pashley, "Red, green, and blue LED based white light generation: issues and control," in *Conference Record of the Industry Applications Conference, 2002. 37th IAS Annual Meeting*, Vol. 1, pp. 327–333, IEEE, Pittsburgh, Pennsylvania (2002).
29. S. Muthu, F. J. P. Schuurmans, and M. D. Pashley, "Red, green, and blue LEDs for white light illumination," *J. Sel. Top. Quantum Electron.* **8**(2), 333–338 (2002).
30. B. Jones, C. M. Hesford, and C. E. Cooper, "The use of portable NIRS to measure muscle oxygenation and haemodynamics during a repeated sprint running test," *Adv. Exp. Med. Biol.* **789**, 185–191 (2013).
31. S. T. Aspenes and T. Karlsen, "Exercise-training intervention studies in competitive swimming," *Sports Med.* **42**(6), 527–543 (2012).
32. H. M. Toussaint, "Differences in propelling efficiency between competitive and triathlon swimmers," *Med. Sci. Sports Exerc.* **22**(3), 409–415 (1990).
33. R. A. Jacobs et al., "Improvements in exercise performance with high-intensity interval training coincide with an increase in skeletal muscle mitochondrial content and function," *J. Appl. Physiol.* **115**(6), 785–793 (2013).
34. D. V. Van Wyk and M. I. Lambert, "Recovery strategies implemented by sport support staff of elite rugby players in South Africa," *S. Afr. J. Physiother.* **65**(1), 1–6 (2009).
35. C. M. Bleakley and G. W. Davison, "What is the biochemical and physiological rationale for using cold-water immersion in sports recovery? A systematic review," *Br. J. Sports Med.* **44**(3), 179–187 (2010).
36. O. Yanagisawa et al., "Effects of cooling on human skin and skeletal muscle," *Eur. J. Appl. Physiol.* **100**(6), 737–745 (2007).
37. M. Ihsan et al., "Influence of post-exercise cooling on muscle oxygenation and blood volume changes," *Med. Sci. Sports Exerc.* **45**(5), 876–882 (2013).
38. A. Barnett, "Using recovery modalities between training sessions in elite athletes: does it help?," *Sports Med.* **36**(9), 781–796 (2006).

Ben Jones obtained a BSc degree in sport and exercise science (DeMontfort University, UK, 2005) and an MS degree in sport health sciences (Life, USA, 2011). A PhD candidate at the University of Essex since 2011, he has published papers on oxygen transport and muscle damage and recovery. His current research projects include: developing noninvasive optical tools to measure oxygen utilization and blood flow in sports science; and using hypoxia as a training tool in elite athletes.

Marco Dat obtained an MSc degree in medical engineering (Eindhoven University of Technology, The Netherlands, 2010). He works as an application specialist of near-infrared spectroscopy equipment at Artinis Medical Systems B.V. in Elst, The Netherlands, since 2010. His activities include providing scientific information and assistance to users, as well as product innovation.

Chris E. Cooper obtained a BSc degree in biochemistry (Bristol, UK, 1985) and a PhD degree in biophysics (Guelph, Canada, 1989). A full professor at the University of Essex since 1999, he has published 170 papers on oxygen transport and metabolism in biology and medicine. His current research projects include developing noninvasive optical tools to measure oxygen utilization and blood flow in clinical medicine and sports science; and using synthetic biology tools to develop an artificial oxygen carrying blood substitute.